Redox Biology 24 (2019) 101222

Contents lists available at ScienceDirect

Redox Biology

journal homepage: www.elsevier.com/locate/redox

HDL subclass proteomic analysis and functional implication of protein dynamic change during HDL maturation

Yuling Zhang[a,b,d], Scott M. Gordon[c,e], Hang Xi[b], Seungbum Choi[b], Merlin Abner Paz[b], Runlu Sun[a,d], William Yang[b], Jason Saredy[b], Mohsin Khan[b], Alan Thomas Remaley[c], Jing-Feng Wang[a,d], Xiaofeng Yang[b], Hong Wang[b,*]

[a] Cardiovascular Medicine Department, Sun Yat-sen Memorial Hospital, Sun Yat-sen University, Guangzhou, 510120, China
[b] Centers for Metabolic & Cardiovascular Research, Department of Pharmacology, Temple University School of Medicine, Philadelphia, PA, 19140, USA
[c] Cardiopulmonary Branch, NHLBI, National Institutes of Health, Building 10 Room 2C433, Bethesda, MD, 20892, USA
[d] Guangdong Province Key Laboratory of Arrhythmia and Electrophysiology, Guangzhou, China
[e] Saha Cardiovascular Research Center, University of Kentucky, Lexington, KY, 40536, USA

ARTICLE INFO

Keywords:
Cardiovascular disease
Lipids and cholesterol
Proteomics
Metabolism
Risk factors

ABSTRACT

Recent clinical trials reported that increasing high-density lipoprotein-cholesterol (HDL-C) levels does not improve cardiovascular outcomes. We hypothesize that HDL proteome dynamics determine HDL cardioprotective functions. In this study, we characterized proteome profiles in HDL subclasses and established their functional connection. Mouse plasma was fractionized by fast protein liquid chromatography, examined for protein, cholesterial, phospholipid and trigliceride content. Small, medium and large (S/M/L)-HDL subclasseses were collected for proteomic analysis by mass spectrometry. Fifty-one HDL proteins (39 in S-HDL, 27 in M-HDL and 29 in L-HDL) were identified and grouped into 4 functional categories (lipid metabolism, immune response, coagulation, and others). Eleven HDL common proteins were identified in all HDL subclasses. Sixteen, 3 and 7 proteins were found only in S-HDL, M-HDL and L-HDL, respectively. We established HDL protein dynamic distribution in S/M/L-HDL and developed a model of protein composition change during HDL maturation. We found that cholesterol efflux and immune response are essential functions for all HDL particles, and amino acid metabolism is a special function of S-HDL, whereas anti-coagulation is special for M-HDL. Pon1 is recruited into M/L-HDL to provide its antioxidative function. ApoE is incorporated into L-HDL to optimize its cholesterial clearance function. Next, we acquired HDL proteome data from Pubmed and identified 12 replicated proteins in human and mouse HDL particle. Finally, we extracted 3 shared top molecular pathways (LXR/RXR, FXR/RXR and acute phase response) for all HDL particles and 5 top disease/bio-functions differentially related to S/M/L-HDL subclasses, and presented one top net works for each HDL subclass. We conclude that beside their essencial functions of cholesterol efflux and immune response, HDL aquired antioxidative and cholesterol clearance functions by recruiting Pon1 and ApoE during HDL maturation.

1. Introduction

Epidemiologic studies have demonstrated that low high-density lipoprotein-cholesterol (HDL-C) levels are a predictor of cardiovascular disease (CVD) [1]. However, clinical trials reported that HDL-C elevation did not improve cardiovascular outcomes [2]. HDL is not only a carrier of cholesterol for cellular cholesterol efflux and uptake but also a complex of lipoproteins containing many proteins and other lipids that influence HDL functions.

HDL is composed of a cholesterol core enriched with cholesterol ester (CE) and triglyceride (TG), and surface lipid bilayer containing free cholesterol (FC), phospholipid (PL) and proteins. Compared with other lipoproteins, HDL is highly heterogeneous in size, charge and composition, which are modified during HDL maturation from small to

Abbreviations: S-HDL, Small high-density lipoprotein; M-HDL, Medium high-density lipoprotein; L-HDL, Large high-density lipoprotein; FPLC, Fast protein liquid chromatography; CVD, Cardiovascular disease; CETP, Cholesterol ester transport protein; MS, Mass Spectrometry; ABCA1, ATP-binding cassette transporter 1; SR-BI, Scavenger receptor class B member 1; RCT, Reverse cholesterol transport; TC, Total cholesterol; TG, Total triglyceride; PL, Phospholipid; CSH, Calcium silica hydrate; AB, Ammonium bicarbonate; LXR, The liver X receptor; RXR, The retinoid X receptor; FXR, The bile acid receptor

* Corresponding author.
E-mail address: hongw@temple.edu (H. Wang).

https://doi.org/10.1016/j.redox.2019.101222
Received 22 April 2019; Received in revised form 9 May 2019; Accepted 14 May 2019
Available online 17 May 2019

large HDL, This maturaturation process orchestrates reverse cholesterol transport (RCT). HDL particles are usually divided into three subclasses based on their size as small, medium and large (S, M, and L)-HDL. These HDL subclass maybe different in their chemical and biological properties [3–5]. It was proposed that S-HDL primarily interacts with ABCA1 to mediate the efflux of cholesterol from peripheral cells, while L-HDL interacts with SR-BI and ABCG1 to deliver cholesterol to the liver [6–9].

The understanding of HDL heterogeneity has greatly increased with the progressive development of analytical technologies (Supplemental Table 1). Difference in HDL density (1.063–1.210 g/mL) was first recognized by gradient ultracentrifugation [10]. The first two HDL protein moieties, later known as ApoA1 and ApoA2, were identified in the late 1960s using early electrophoresis methods [11]. Soon after, ApoE was found in light/S-HDL, and ApoD was found in more dense/L-HDL fractions [12,13]. Improvements in SDS-PAGE technology in the early 1980s revealed serum amyloid A (Saa) and ApoA4 in human HDL [14]. It was reported that 90% of plasma Pon1 is associated with ApoA1 and present in HDL [15]. Approximately 200 distinct proteins were identified in HDL by different laboratories using mass spectrometry (MS) technology [16–20], which permitted further exploration of HDL protein heterogeneity. Dr. Davidson reported 28 HDL proteins distributed across five human HDL subpopulations (HDL2b, 2a, 3a, 3b and 3C), identified by isopycnic density ultracentrifugation, and described correlations among ApoL1, Pon1 and Pon3 functions to protect LDL oxidation [21]. However, differential HDL proteomic analysis among HDL subgroups has been limited, and systemic comparisons of HDL proteomes across species have not been performed.

Unlike humans, detailed studies of the mouse lipoproteome are scarce. Mice have significantly different lipid metabolism than humans. For instance, they lack cholesteryl ester transfer protein (CETP), which transfers CE from HDL to LDL and very-low-density lipoproteins (VLDL) in humans. Thus, mice carry the majority of plasma cholesterol in HDL, while humans carry much of it in LDL [22]. Therefore, mice have an inherent advantage in resisting the development of atherosclerosis, explaining the difficulty in establishing atherosclerotic mouse models using genetic knockout methods. Although there are differences between the mouse and human lipoproteomes, mice share more similarities with humans. Using gel filtration chromatography and MS analysis, Scott M. identified 113 lipid-associated proteins in mice and compared the mouse lipoproteome and its size distribution to a previous human analysis. He demonstrated that protein diversity in the LDL and HDL size ranges was similar in mice and humans, although some distinct differences were noted. Furthermore, whether a given protein was associated with L-versus S-HDL subclasses was also similar between species [23]. A better understanding of the proteomic composition of mouse lipoproteins may offer additional explanations and provide a stronger rationale for the use of mice to study human atherosclerotic disease.

The purpose of this study used FPLC to identify differential HDL proteomics in the S/M/L-HDL subclasses, try to make HDL subclasses oversimplified and establish a subclasses proteomic feasible research model, and also try to discover potential functional pathways of these HDL subgroups, as determined by their protein heterogeneity.

2. Experimental procedures

2.1. Mouse model and plasma collection

ᅳ C57BL/6J male mice were used in this study. Animal studies were approved by the Temple University Institutional Animal Care and Use Committee (IACUC). Mice were fed a standard rodent chow (0% cholesterol, 5.23% fat, 0.37% methionine, 2.39 mg/g choline, 3.19 mg/kg folate, 54.6 μg/kg B12, 14.5 mg/kg B6, cat# 8640, Harlan Teklad, Madison, WI) and fasted overnight. Blood sample was collected when mice were at the age of 14–16 weeks by cardiac puncture and citrate anticoagulation. Plasma were isolated in a tabletop centrifuge at ~1590 g for 15 min at room temperature and pooled from 3 mice. The pooled plasma was stored at 4 °C.

2.2. Lipoprotein measurement and S/L/M-HDL fractions isolation

HDL particles were fractionated as described [17]. Briefly, 450 μL of pooled plasma was applied to a Superdex 200 gel filtration column (10/300 GL, GE Healthcare) in an ÄKTA fast protein liquid chromatography (FPLC) system, and separated at a flow rate of 0.3 mL/min in standard Tris buffer (10 mM Tris, 0.15 M NaCl, 1 mM EDTA). 48 fractions were collected (GE Healthcare) and stored at 4 °C.

FPLC fractions were tested for lipid and total protein concentrations by using Colorimetric kits and bicinchoninic acid (BCA). Protein content of lipoprotein fractions were quantified by the absorbance at OD280. Total cholesterol (TC) and triglyceride (TG) levels were assayed by Colorimetric kits. Phospholipid (PL) levels were assessed by using enzymatic kits from Wako Diagnostics (Richmond, VA). Fractions 10 to 15 were determined as VLDL by high content of TG, 16 to 22 as LDL by the lower protein peak, 25 to 36 as HDL by higher PL and TC content, and 37 to 45 as albumin. HDL fractions were evenly clustered into 3 pools according to particle size, fractions 25 to 28 as large-HDL particles (L-HDL), 29 to 32 as medium-HDL (M-HDL), and 33 to 36 as small-HDL (S-HDL). Total protein concentration in small, medium and large (S/M/L)-HDL fractions were assessed by BCA assay. Total PL, cholesterol, and TG in S/L/M-HDL fractions were normalized by protein content in each fraction.

2.3. Mass spectrometry analysis of S/L/M-HDL fractions

The pooled S/L/M-HDL fractions were then purified for PL measurenment by using a calcium silica hydrate (CSH) resin as described [17]. Briefly, 400 μL each fraction had 45 μg of CSH added, mixed gently for 30 min at room temperature, and pelleted by centrifugation (~2200 × *g* for 2 min). Supernatant containing lipid-free plasma proteins was removed and the remaining CSH pellet was washed with 50 mM ammonium bicarbonate (AB).

These PL containting components of each pooled fraction were then subjected to mass spectrometry (MS) analysis using a Qstar XL-MS system [24]. In brief, HDL particles were digested with trypsin while still bound to the CSH. Sequencing grade trypsin (1.5 μg in 25 μL of 50 mM AB) was added to each CSH pellet and incubated at 37 °C overnight on a rotating plate. To collect the digested peptides, the CSH was washed with 125 μL of 50 mM AB. Eluted peptides were first reduced and then carbamidomethylated with dithiothreitol (200 mM 30 min at 37 °C) and iodoacetamide (800 mM 30 min at room temperature), respectively. Peptides solutions were then lyophilized to dryness and stored at −20 °C until analyzed by MS.

Dried peptides were reconstituted in 15 μL of 0.1% formic acid in water. An Agilent 1100 series auto-sampler/HPLC was used to draw 0.5 μL of sample and inject it onto a C18 reverse phase column (GRACE 150 × 0.500 mm) where an acetonitrile concentration gradient (5–30% in water with 0.1% formic acid) was used to elute peptides for online ESI-MS/MS by a QStar XL mass spectrometer. Column cleaning was conducted automatically with 2 cycles of a 5–85% acetonitrile gradient lasting 15min each between runs.

To identify the protein composition of lipid containing particles, peak lists generated from analysis of each fraction were scanned against the Swiss-Prot Protein Knowledgebase for Mus musculus (release 2011, 533657 sequences) using Mascot (ver. 2.2.07) and X! Tandem (ver. 2010.12.01.1) search engines. Scaffold software (ver. Scaffold_4.3.4, Proteome software) was used to validate MS based peptide and protein identifications. Since equal volumes of sample were applied to the MS analysis, the relative amount of given protein present in a given fraction is proportional to the number of special counts in each fraction. This method provides a semi quantitative abundance pattern across each fraction as immunological analysis [25]. The MS proteomics data have

been deposited to the ProteomeXchange Consortium via the PRIDE partner repository with the dataset identifier PXD011185. It will become accessible via http://www.proteomexchange.org. upon the manuscript publication.

2.4. Classification of FPLC-MS identified proteins in mouse HDL

Abbreviation and Uniprot ID of MS identified proteins in S/L/M-HDL were abtained from public databases (Genecards and Uniprot). Protein was classified according to their biological function described in Pathcards Pathway Unification Data Base. Because many of the immunoglobulins discussed do not have abbreviations in Genecards, we used their full protein name.

2.5. Comparison of HDL protein abundance between mouse S/L/M-HDL

HDL protein abundance was compared between mouse S/L/M-HDL particles based on relative abundance of MS identified peptide counts. A value of 1.0 was assigned to the highest peptide count of each specific protein in each HDL fractions. Peptide counts for other proteins were scaled accordingly and presented as Heat map. Next, we identified overlapped proteins in three S/L/M-HDL subclass and presented as Venn-diagram. Finally, fold value of peptide counts in L-HDL was calculated by dividing that in S-HDL. Positive numbers describe the fold changes of increased proteins in L-HDL. Negative numbers describe the fold changes of decreased proteins which and was derived by dividing negative one (-1) by the fold value.

2.6. Identification of HDL proteins dynamic change in mouse S/L/M-HDL

HDL protein dynamic changes (increase or decrease during HDL maturation) from S-HDL to L-HDL were grouped by database-defined biological functions and graphed on their relative abundance value.

2.7. Identification of replicated proteins in human and mouse HDL and their dynamic changes

Replicated proteins in human and mouse HDL were identified by comparing our mouse HDL proteomics data with published HDL proteomics data of human and mouse available in PubMed from 2010 to 2015. Among 276 reported human HDL proteins, only 93 were reported 2 times or more and were selected for analysis. There were only 2 mouse HDL proteomics reported during this period of time, with only 19 out of 111 replicated in both publications.

Dynamic changes of the identified replicated proteins in human and mouse HDL were grouped by whether they increased or decreased during HDL maturation, and graphed on their relative abundance value.

2.8. Identification and comparison of ingenuity pathways and disease/bio-functions of identified S/M/L-HDL proteins (IPA software)

In order to explore HDL functional diversity derived from HDL protein dynamic changes, we identified ingenuity pathways and disease/bio-functions of the 51 identified HDL protein in S/L/M-HDL using Ingenuity Pathway Analysis (IPA) software (www.ingenuity.com).

The significance of identified pathways and disease/bio-functions were evaluated by *p*-value which described the significane of individual pathways over others in each HDL fraction. The number of HDL proteins over the total previously identified proteins are described as overlaps with percentage. Overlap describes the number of identified HDL protein overlaps with the listed pathway molecules. The significance comparison of Ingenuity pathways and disease/bio-functions between the three HDL fractions was calculated as *p* value using IPA software.

2.9. Identification of top scored networks and related diseases/bio-functions of S/L/M-HDL proteins (IPA software)

To investigate whether S/L/M-HDL proteins were related to the diversity bio-functions of HDL in RCT, predicted networks of S/L/M-HDL proteins were identified via their interconnected molecules using IPA software. IPA score are calculated using the IPA algorithm. Network-related diseases/bio-functions were solicited also using IPA software.

2.10. Experimental design and statistical rationale

For the investigation of HDL cardioprotective functional signatures, in S/M/L HDL fractions respectively, WT mouse plasma was applied to FPLC, and divided into 47 fractions totally. HDL particles characterized by their high PL content were enriched in fractions 25–36. In order to improve methodological sensitivity, we pooled three plasma samples together to decrease coefficient of variation of the mean, rather than applying technical replicates. We used 3 replicates for statistics in lipoprotein profile and L/M/S-HDL subclass characterization. Results are expressed as the mean ± SEM. Statistical comparison of single parameters between two groups was performed by independent *t*-test. A probability value $p < 0.05$ was considered to be significant. We further evenly divided the HDL fractions into three subclasses according to particle size, fractions 25–28 as large particles, 29–32 as medium, and 33–36 as small, to properly reflect the average/weighted average and more decrease the variation in each of the S/M/L HDL fractions.

2.11. Quantifications

Experimental data was presented as means ± SEM. Differences of statistical significance were determined by one-way analysis of variance (ANOVA) followed by Bonferroni's post hoc test. Statistical significance was defined as a two-tailed probability of less than 0.05. The significance of identified pathway and disease/bio-function analysis between three fractions was calculated as *p* value using IPA software.

3. Results

3.1. Lipoprotein profile and S/L/M-HDL fraction characterization

We determined the content of protein, PL, TC and TG by FPLC fractionation of pooled plasma from male C57/B6 mice (Fig. 1A). We defined the HDL particles for fractions 25–36 based on their high content of PL and TC (Fig. 1C/D), VLDL particles for fractions 10–15 based on their high TG content (Fig. 1E), and distinguished LDL particle for fractions 16–22 (Fig. 1B).

HDL fractions were divided evenly and grouped as L-HDL (fractions 25–28), M-HDL (fractions 29–32) and S-HDL (fractions 33–36). Protein concentration was higher in S-HDL (1.54 ± 0.10 mg/mL), lower in M-HDL (0.36 ± 0.12 mg/mL), and much lower in L-HDL (0.07 ± 0.01 mg/mL)(Fig. 1F). Relative concentration of PL, TC and TG, normalized by protein concentration, appeared to be the lowest in S-HDL (2.18 ± 1.12, 1.13 ± 1.03 and 0.20 ± 0.18 μg/mg), relatively high in L-HDL (24.16 ± 1.14, 13.34 ± 0.73 and 1.52 ± 0.13 μg/mg), and the highest in M-HDL (33.35 ± 2.01, 19.26 ± 2.07 and 1.93 ± 0.10 μg/mg) (Fig. 1G/H/I).

3.2. Proteins identified in mouse L/M/S-HDL particles and their representative biological functions

We detected totally 51 proteins in all S/M/L-HDL subclasses by MS analysis and present the protein name, abbreviation and UniProt ID from public databases in Table 1A. We divided these 51 proteins into 4 biological functional groups. Group 1 lipid metabolism includes 5 proteins (ApoA1, ApoA2, ApoA4, ApoC3, and ApoE). Group 2 contains

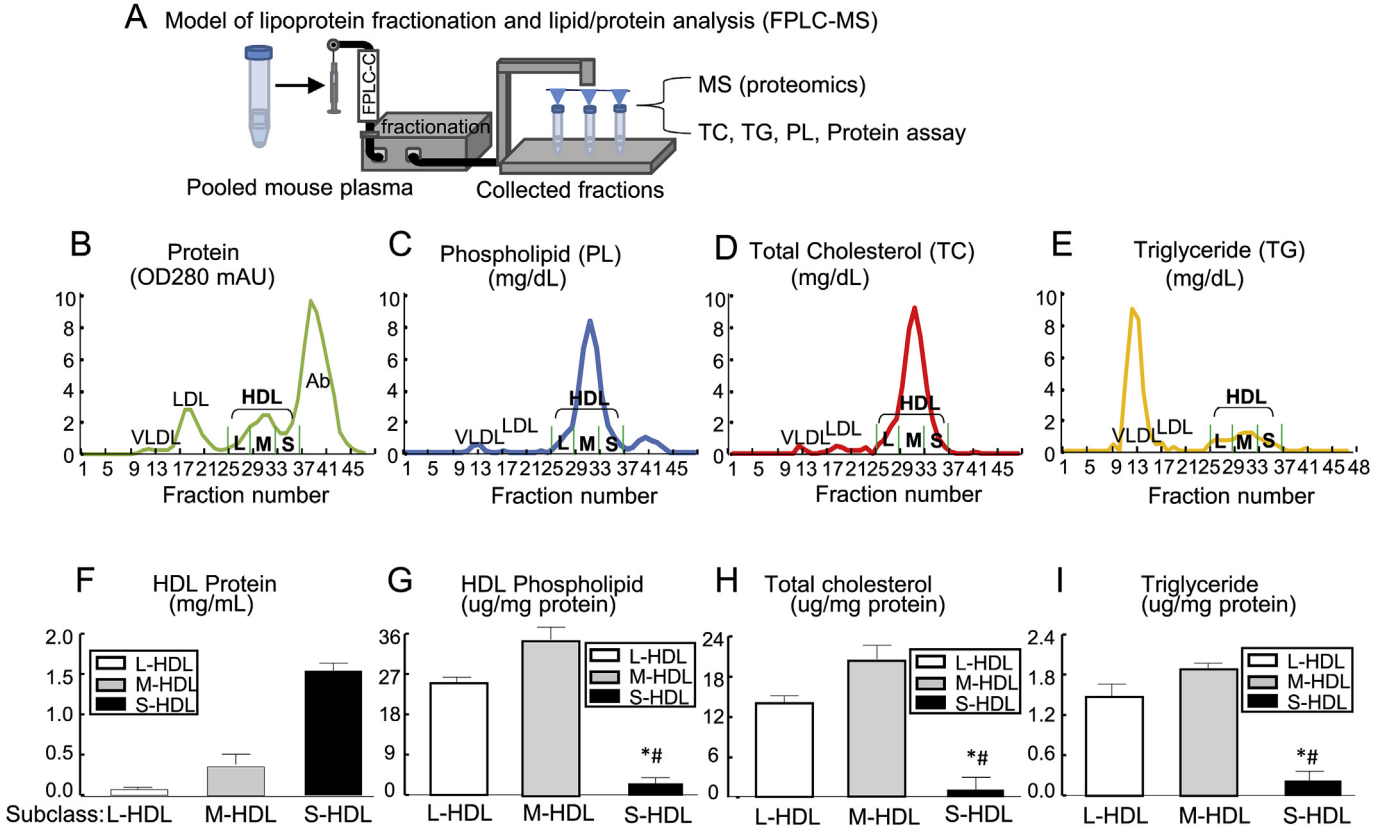

Fig. 1. Lipoprotein profile and L/M/S-HDL subclass characterization of mouse plasma. Blood was collected from male C57BL/6J mice at 14–16 weeks of age. Pooled plasma from 3 mice was applied to a ÄKTA FPLC system for lipoprotein fractionation. Forty-eight fractions were collected and further assessed for phospholipid, cholesterol, and triglyceride concentrations using biochemical kits from Wako. Protein content was quantified by the absorbance at OD280. Fractions 10 to 15 were determined as VLDL by the peak of triglyceride, 16 to 22 as LDL by the peak of protein, 25 to 36 as HDL by the peak of phospholipid, 37 to 45 as albumin. Fractions 25 to 28 were pooled as large-HDL particles (L-HDL), 29 to 32 as medium-HDL (M-HDL), and 33 to 36 as small-HDL (S-HDL). **(A) Model of lipoprotein fractionation and lipid/protein analysis (FPLC-MS). (B) Protein. (C) Phospholipid. (D) Total cholesterol. (E) Triglyceride.** Protein, phospholipid, total cholesterol and triglyceride profiles were established by biochemical assessment in 48 fractions. **(F) HDL protein.** Protein concentrations of pooled L/M/S-HDL fractions were assessed by BCA assay. **(G) HDL phospholipid. (H) HDL total cholesterol. (I) HDL triglyceride.** Phospholipid, total cholesterol and triglyceride content of pooled L/M/S-HDL fractions were assessed and normalized by HDL protein concentration. HDL, high density lipoprotein; LDL, low density lipoprotein; VLDL, very low density lipoprotein. BCA, bicinchoninic acid. *p < 0.05 compared with L-HDL, #p < 0.05 compared with M-HDL.

25 immune response proteins, including 3 subgroups such as complement (10 proteins; C3, C4B, C5, C8A, C8B, C8G, CFB, CFH, CFI, and Clu), immunoglobulins (7 proteins; Igcab, Igfals, Igg2B, Ighg3, Igkc, Igγ-1, and Lac-1), and inflammation (7 proteins; Hla-B, Ambp, Pon1, Saa4, ItiH1, ItiH3, and ItiH4). Group 3 coagulation (7 proteins; F2, F10, Klkb1, Kng, Serpina10, Serpinf2, and Serping1). Group 4 has 14 other proteins (Ahsg, Alb, CpN1, CpN2, Afm, EGFR, Fn1, Gpld1, CP, Lifr, Mug1, and Vtn)(Table 1B).

3.3. Identification of protein overlaps in mouse HDL subclasses

We presented abundance of MS identified protein from S/M/L-HDL subclasses based on peptide counts in Fig. 2A/B. S-HDL contains 39 proteins, and 26 of these have the highest abundance index of 1.0. M-HDL contains 27 proteins, of which 10 have abundance index of 1.0. L-HDL contains 29 proteins, of which 15 have abundance index of 1.0. During the maturation of HDL particles, 18 of 39 S-HLD proteins are absent in M-HDL, 6 more are absent in L-HDL. The M-HDL subclass recruited 9 new proteins, of which 3 are absent in L-HDL. The L-HDL subclass also recruited 9 new proteins. We identified 11 common HDL proteins in all S/M/L-HDL fractions, including Ambp, ApoA1, ApoA2, ApoA4, ApoE, C3, C4B, Clu, Kng1, Saa4, and Mug1 (Figure 2B), 7 L-HDL-specific proteins (CFH, CpN1, CpN2, Fn1, Gpld1, Hba, and Hla-B), 3 M-HDL-only proteins (ItiH3, Serpina10,and Serping1) and 16 unique S-HDL proteins (Afm, Ahsg, C8A, C8B, C8G, CFB, CFI, F10, F2, Hpx, Igfals, Ighg3, Igγ-1, Lac1, Serpinf2,and Vtn) (Fig. 2A/B).

We calculated fold changes by comparing that in L-HDL vs S-HDL (Fig. 2C). ApoE was increased by 39.48-fold, Mug1 by 15.23-fold and Ambp by 12.01-fold. Thirteen proteins were only presented in L-HDL (∞). In contrast, C3 was reduced by 57.63-fold, Clu by 41.49-fold and ApoA1 by 1.55-fold in L-HDL. Twenty-one proteins were absent only in L-HDL(-∞).

3.4. Dynamic protein distribution in mouse HDL subclasses by biological function groups

HDL protein dynamic were characterized by 4 biological function groups defined in Table 1B. Fig. 3-A/B/C/D each present one group and divided into increased or decreased from S-HDL towards the maturation to M/L-HDL. Among lipid metabolism-related proteins, ApoE was increased, ApoA1/2 and ApoC3 were nearly steadily expressed, and ApoA4 was slightly decreased in L-HDL (Fig. 3A). Immune response-related proteins were divided into 3 subgroups. The complement proteins C5 and CFH were increased, while C3, C4B, C8A, C8B, C8G, CFB, CFI and Clu were decreased in L-HDL (Fig. 3B1). The inflammation-related proteins Ambp, Hla-B, ItiH1, ItiH2, and Pon1 were increased, but ItiH3, ItiH4, and Saa4 were decreased (Fig. 3B2). Interestingly, all identified immunoglobulin proteins were decreased in L-HDL (Fig. 3B3). The coagulation related proteins Klkb1, Kng, Serpina10 and Serping1 exhibited an increased pattern, but Serpinf2, F10 and F2 were

Table 1

Proteins identified in mouse L/M/S-HDL particles and their representative biological functions. Pooled mouse plasma fractionated using an ÄKTA FPLC system. Large, medium, small HDL particles were collected as described in Fig. 1 and subjected to proteomic analysis. **(A) Identified HDL proteins; 51 proteins were identified in HDL particles by MS and listed.** The abbreviation and Uniprot ID of the proteins were obtained from public databases (Genecards and Uniprot). **(B) Biological function of HDL proteins;** 51 identified HDL proteins are presented by four relevant biological function groups based on classification in the literature and multiple databases as described in Material and Methods.

A proteins identified in mouse L/M/S-HDL particles(51 proteins, FPLC-MS)

Protein name	Abbreviation	Uniprot ID	Protein name	Abbraviation	Uniprot ID	Protein name	Abbraviation	Uniprot ID
Afamin	Afm	O89020	Epidermal GF-R	EGFR	Q01279	Inter- α trypsin inhibitor chain H2	ItiH2	Q61703
α-2-HS-glycoprotein	Ahsg	P29699	Coagulation factor X	F10	O88947			
Albumin	Alb	P07724	Prothrombin	F2	P19221	Inter- α trypsin inhibitor chain H3	ItiH3	Q61704
α-1-microglobulin	Am bp	Q07456	Fibronectin	Fn1	P11276			
Apolipoprotein A-I	ApoA1	Q00623	Phosphatidylinositol-glycan- specific phospholipase	Gpldl	O70362	Inter- α trypsin inhibitor chain H4	ItiH4	A6X935
Apolipoprotein A-II	ApoA2	P09813	Hemoglobin subunit-α H2 class I	Hba	P01942			
Apolipoprotein A-IV	ApoA4	P06728	Histocompatibility antigen,Q10 α chain	Hla-B	P01898	kallikrein	Klkbl	P26262
Apolipoprotein C-III	ApoC3	P33622	Hemopexin	Hpx	Q91X72	Kininogen-1	Kng	008677
Apolipoprotein E	ApoE	P08226	Ig-γ-2A chain C region secreted form	Igcab	P01864	Ig-λ −1 chain C region	Lac1	P01843
Complement C3	C3	P01027	Insulin-like GF binding protein complex acid labile subunit	Igfals	P70389	Leukemia inhibitory factor receptor	Lifr	P42703
Complement C4–B	C4B	P01029	Ig-γ-2B chain C region	lgg2B	P01867			
Complement C5	C5	P06684	Ig-γ-3 chain C region	Ighg3	P03987	Murinoglobulin-1	Mug1	P28665
Complement C8A	C8A	Q8K182	Ig-κ chain C region	IgkC	P01837	Paraoxonase	Poni	P52430
Complement C8	C8B	Q8BH35	Ig γ-1 chain C region, membrane bound form	Igγ −1	P01869	Amyloid A-4	Saa4	P31532
Complement C8G	C8G	Q8VCG4	Inter- α trypsin inhibitor chain H1	ItiH1	Q61702	Protein Z-dependent protease inhibitor	SerpinalO	Q8R121
Complement factor B	CFB	P04186						
Complement factor H	CFH	P06909				A-2-antiplasmin	Serpinf 2	Q61247
Complement factor I	CFI	Q61129				Plasma protease C1 inhibitor	Serpingl	P97290
Clusterin	Clu	Q06890						
Ceruloplasmin	CP	Q61147				Vitronectin	Vtn	P29788
Carboxypeptidase N catalytic chain	CpN1	Q9JJN5						
Carboxypeptidase N subunit 2	CpN2	Q9DBB9						

B Biological functions of identified mouse L/M/S-HDL proteins

1. Lipid Metabolism (5 proteins)	ApoA1, ApoA2, ApoA4, ApoC3, ApoE
2. Immune Response (25 proteins)	
Compliment	C3, C4B, C5, C8A, C8B, C8G CFB, CFH, CFI, Clu
Immunoglobulin	Igcab Igfals, lgg2B, Ighg3 Igkc, lgγ-1, Lac-1
Inflammation	Hla-B, Ambp, ItiH1, ItiH2, ItiH3, ItiH4, Pon1, Saa4
3. Coagulation (7 proteins)	F2, F10, Klkbl, Kng Serpina10, Serpinf2 Serping1
4. Other (14 proteins)	Ahsg, Alb, CpN1, CpN2, Afm EGFR, Fn1, Gpldl, Hba, CP, Hpx, Lifr, Mug1, Vtn

decreased in L-HDL (Fig. 3C). Finally, in the other type protein group, CpN1, CpN2, Fn1, Gpld1, Hba, Lifr and Mug1 were increased, whereas Ahsg, CP, EGFR, Hpx, Vtn and Afm were decreased in L-HDL (Fig. 3D).

3.5. Model of protein composition change during HDL biosynthesis/maturation

We established a model to describe transition points when HDL proteins join or leave HDL subclasses during HDL biosynthesis/maturation. We found that all S/M/L-HDL contains ApoA1/2/4 and ApoC3 proteins, and ApoE joined only in L-HDL. From S-HDL-to M-HDL, 17 proteins departured 11 joined. From M-HDL to L-HDL, 10 proteins departured M-HDL and 8 joined. Furthermore, we distinguished functions of each S/M/L-HDL subclass based on that of their protein components. S-HDL proteins are primarily associated with cholesterol efflux, the immune response, and amino acid metabolism. M-HDL proteins are more closely associated with cholesterol efflux, the immune response/anti-inflammation, and antioxidation/anticoagulation. L-HDL proteins are more closely associated with cholesterol efflux/clearance, the immune response/anti-inflammation, and antioxidation (Fig. 3E).

3.6. Identification of replicated proteins in human and mouse HDL

We compared our data with published HDL proteomics datasets (10 human HDL and 2 mouse HDL proteomics) (Fig. 4A/B). Among 276 proteins identified in human HDL, we identified 93 replicated proteins (reported ≥ 2 times). Among 111 mouse HDL proteins identified by others, 19 are replicated (details in Supplemental Table 2). Finally, we identified 12 replicated proteins among all published humans/mouse and our mouse HDL proteins (replicated ≥3 times). We presented the distribution pattern of these 12 replicated HDL proteins in S/M/L-HDL subclasses in Fig. 4C. During HDL maturation, Among these 12 replicated HDL proteins, three proteins (PON1, C5 and ApoE) increased, 4

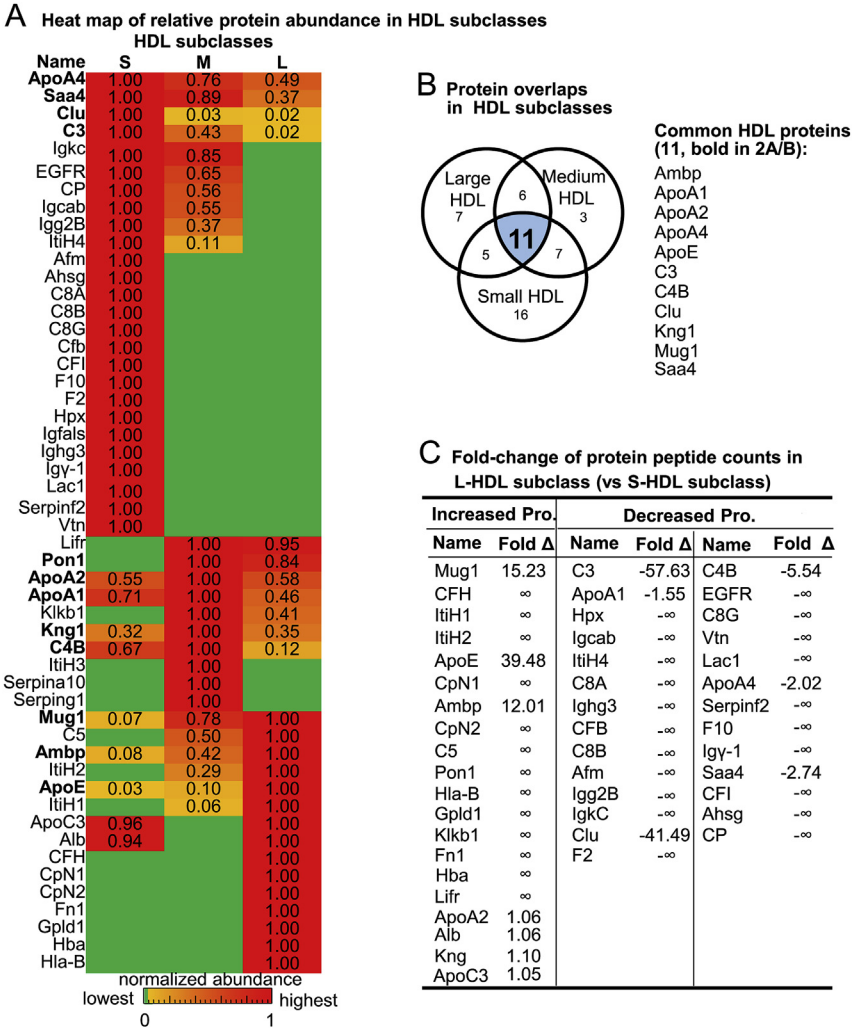

C Fold-change of protein peptide counts in L-HDL subclass (vs S-HDL subclass)

Increased Pro.		Decreased Pro.			
Name	Fold Δ	Name	Fold Δ	Name	Fold Δ
Mug1	15.23	C3	-57.63	C4B	-5.54
CFH	∞	ApoA1	-1.55	EGFR	-∞
ItiH1	∞	Hpx	-∞	C8G	-∞
ItiH2	∞	Igcab	-∞	Vtn	-∞
ApoE	39.48	ItiH4	-∞	Lac1	-∞
CpN1	∞	C8A	-∞	ApoA4	-2.02
Ambp	12.01	Ighg3	-∞	Serpinf2	-∞
CpN2	∞	CFB	-∞	F10	-∞
C5	∞	C8B	-∞	Igy-1	-∞
Pon1	∞	Afm	-∞	Saa4	-2.74
Hla-B	∞	Igg2B	-∞	CFI	-∞
Gpld1	∞	IgkC	-∞	Ahsg	-∞
Klkb1	∞	Clu	-41.49	CP	-∞
Fn1	∞	F2	-∞		
Hba	∞				
Lifr	∞				
ApoA2	1.06				
Alb	1.06				
Kng	1.10				
ApoC3	1.05				

Fig. 2. Identification of protein overlaps in mouse HDL subclasses. Pooled mouse plasma was fractionated using an ÄKTA FPLC system. Large, medium, small HDL subclasses were collected as described in Fig. 1 and subjected to proteomic analysis using a Qstar XL-MS system. 51 proteins were identified in HDL particles and abbreviated according to Genecards website. **(A) Heat map of relative protein abundance in HDL particles.** Relative abundance of each identified protein in HDL particles were described by peptide count, determined by MS. A value of 1.0 was assigned to the highest peptide count of the specific protein in three S/M/L-HDL subclasses. Peptide counts for other proteins were scaled accordingly. The highest values are colored red and gradually changed to yellow for the lower values. Green indicates no peptide was identified in that particular HDL fraction. **(B) Protein overlaps in HDL particle;** Venn-diagram describes the presence of identified protein in HDL particles (39 in S-HDL, 27 in M-HDL, and 29 in L-HDL). 11 proteins overlap in all S/M/L-HDL fractions and are listed as common HDL proteins. **(C) Fold-change of protein peptide counts in L-HDL;** Fold change of each protein in L-HDL was calculated with dividing its peptide count in L-HDL by that in S-HDL. Positive numbers describe the fold changes of increased proteins in L-HDL. Negative numbers describe the fold changes of decreased proteins derived from dividing negative one (−1) by the fold value. Infinity symbol "∞" indicates protein present in L-HDL but absent in S-HDL., whereas, "-∞" indicates protein absent in L-HDL but present in S-HDL. Protein name abbreviation are explained in Table 1A. (For interpretation of the references to color in this figure legend, the reader is referred to the Web version of this article.)

proteins (ApoA1, ApoA2, ApoC3, and KNG1) nearly steadily expressed, and 5 proteins (C3, SAA4, VTN, CP, and ApoA4) largely reduced.

3.7. Identification of ingenuity pathways and disease/bio-functions of HDL subclasses and significance comparison

Using pathway identification strategies and IPA software, we determined Ingenuity pathways and disease/bio-functions related to the 51 mouse HDL proteins we identified in this study. S-HDL fractions were most likely related to the regulation of 3 top Ingenuity pathways (LXR/RXR activation, FXR/RXR activation, and acute phase response) (Fig. 5B) and 5 top bio-function groups (complement activation, organ inflammation, hemolysis, cytolysis and inflammation)(Fig. 5C). Among the 39 identified mouse S-HDL proteins, 35.9–38.5% and 20.5–46.2% are involved in these Ingenuity pathways and disease/bio-function groups, respectively. M-HDL fractions were most likely related to 3 Ingenuity pathways (LXR/RXR activation, FXR/RXR activation and acute phase response) and 5bio-function groups (complement activation, inflammation, acute coronary syndrome, PL efflux and myocardial infarction), involving 40.7–55.6% and 25.9–55.6% of the identified M-HDL proteins, respectively. L-HDL fractions are most likely related to 3 Ingenuity pathways (LXR/RXR activation, FXR/RXR activation and acute phase response) and 5 top bio-function groups (complement activation, cholesterol efflux/metabolism, PL efflux, vascular disease and lipid homeostasis/transport), involving 34.5–41.4% and 17.2–44.8% of the identified L-HDL proteins, respectively. Via significance comparison, we found that S-HDL proteins favor LXR/RXR and FXR/RXR activation, acute phase response, complement system, coagulation system, inflammation and lipid metabolism, and L-HDL proteins were more closely related to clathrin-mediated endocytosis, atherosclerosis, macrophage IL-12 production and cholesterol efflux (Fig. 5D/E).

3.8. Network identification of HDL proteins

We further identified connective networks for each S/M/L-HDL fraction (Fig. 6A/B). We list 3 top S-HDL networks. The first one is for humoral immune/inflammatory responses/carbohydrate metabolism. The second one is for cellular assembly/organization/tissue development/cellular function and maintenance. The first S-HDL network involves 22 our identified protein (56.4% of all network proteins, with 59 IPA score) including the inflammatory molecules Saa, ItiH4, complement C3 and CFB (Fig. 6D). Among the 3 top M-HDL networks, the first one is for developmental & hereditary disorders/immunological disease. The second one is for cell survival/cellular compromise and development. The first M-HDL network involves 21 our identified protein (77.8% of all network proteins, with 59 IPA score) including the thiol protease inhibitor Kng1, the collagen biosynthesis enzyme Klkb1, C3 and the antioxidant Pon1 (Fig. 6E). Among the 3 L-HDL networks, the first one is for cell survival/connective tissue disorders/hematological disease. The second one is for lipid metabolism/small molecule biochemistry/drug metabolism. The first L-HDL network involves 21 our identified protein (72.4% of all network proteins, with 59 IPA score) including ApoA1, ApoA2, ApoA4, and Pon1 (Fig. 6F).

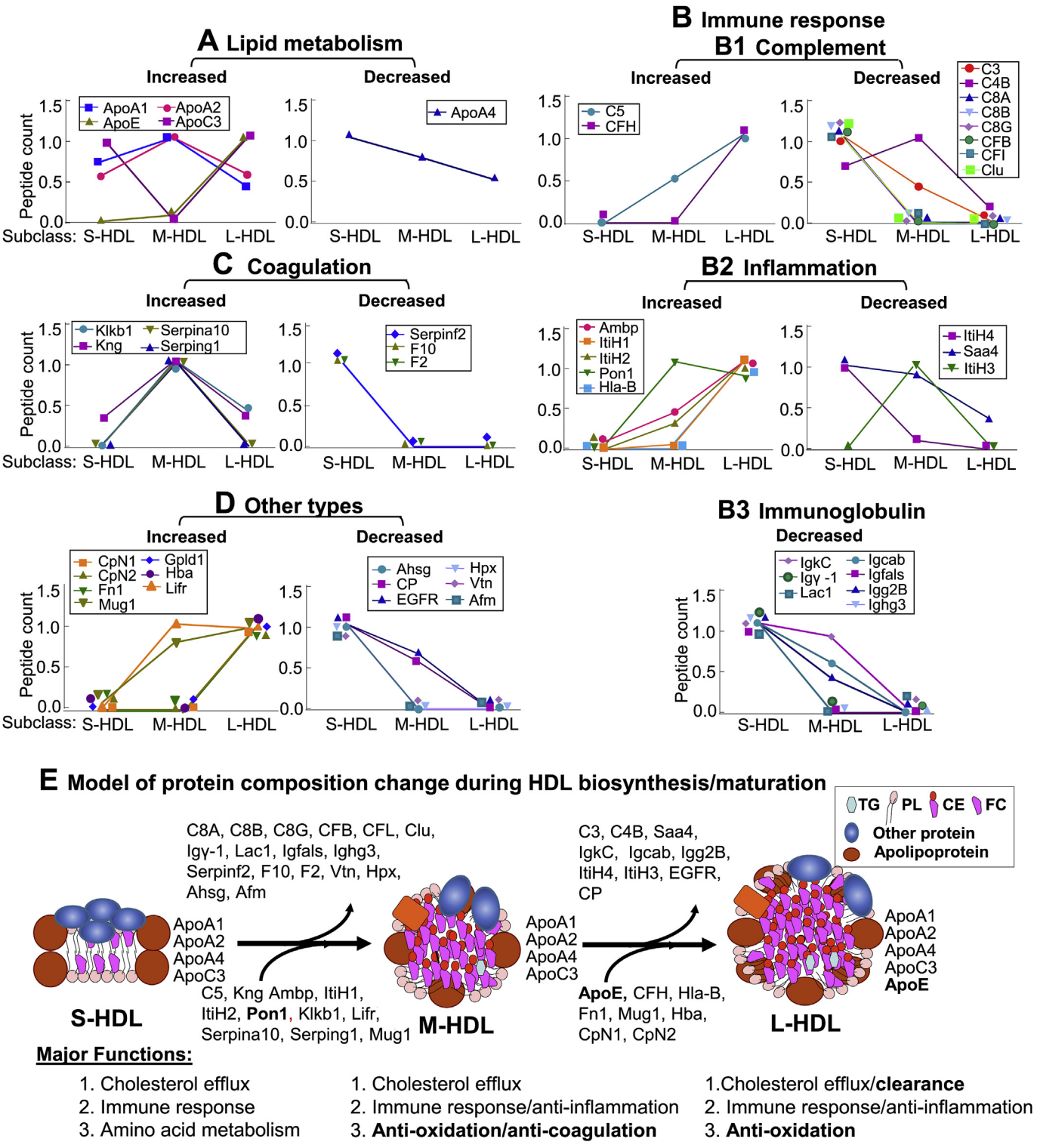

Fig. 3. Dynamic protein distribution in mouse HDL subclasses by biological function groups and model of protein composition change during HDL biosynthesis/maturation. HDL fractions (S/M/L) were collected from FPLC purification as described in Fig. 1. Proteins in each HDL fraction were identified by Qstar XL-MS analysis as describing in Fig. 2. Relative abundance of each identified protein in HDL particles were described by peptide count, determined by MS. A value of 1.0 was assigned to the highest peptide count of the specific protein in three S/M/L-HDL fractions. Identified HDL proteins were grouped by the biological function as describing in Table 1 and classified as increased and decreased groups. Protein dynamic changes are presented as relative peptide count curves. **(A) Lipid metabolism. (B) Immune response; B1, Complement proteins, B2, Inflammatory protein, B3, Immunoglobin proteins. (C) Coagulation proteins. (D) Other types. (E) Model of protein composition change during HDL biosynthesis/maturation.** Flow chat describes transition points when HDL proteins join or departure from HDL subgroups during HDL biosynthesis/maturation. Protein names highlighted in red are those emphasized in the session of discussion. Protein name abbreviation are explained in Table 1A. (For interpretation of the references to color in this figure legend, the reader is referred to the Web version of this article.)

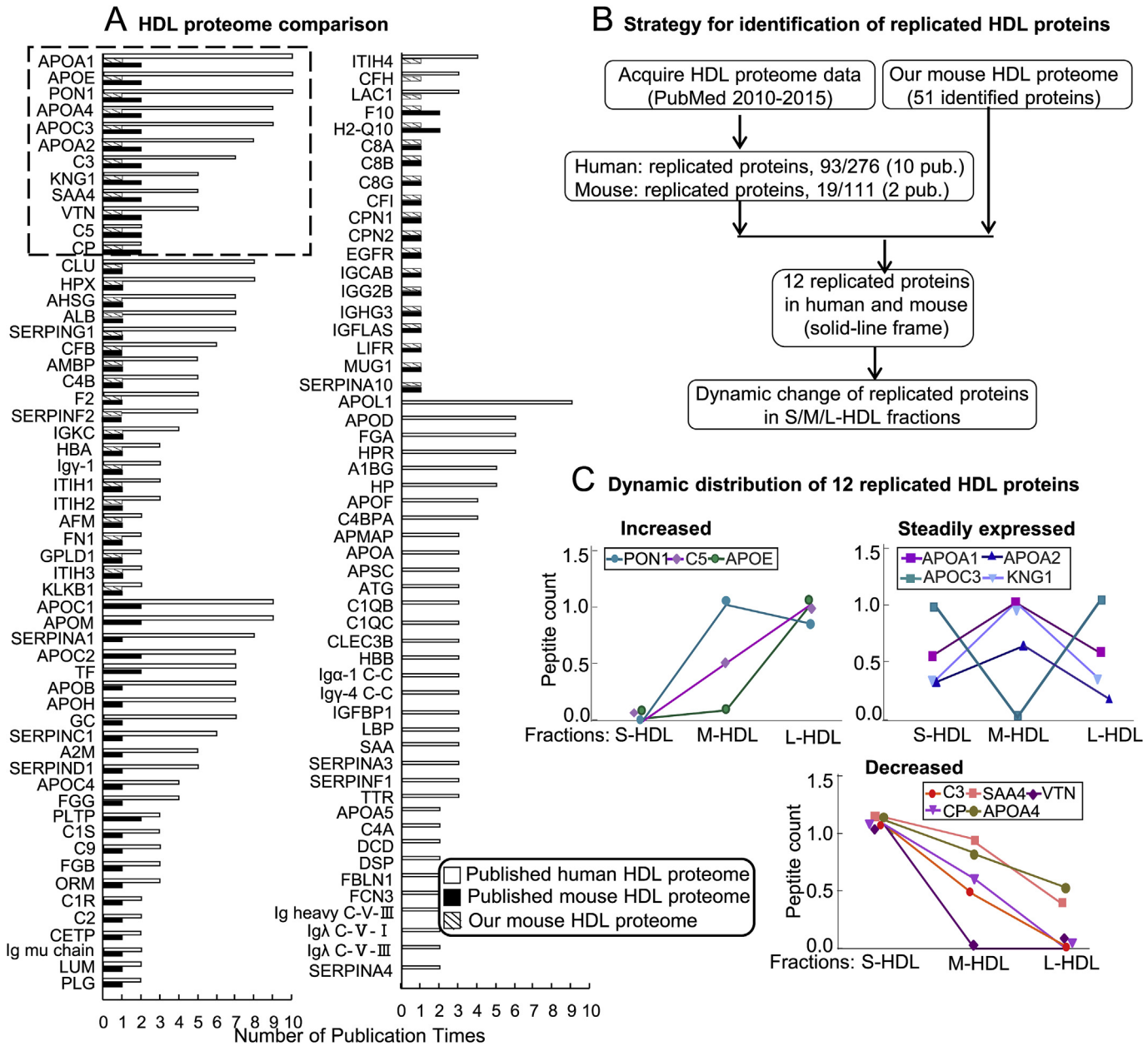

Fig. 4. Identification of replicated proteins in human and mouse HDL. Reported HDL proteomics data was acquired from PubMed database. 14 human and 2 mouse HDL proteomics data were reported (from 2010 to 2015, details in Supplement Table 2), which were compared to our mouse HDL proteome. **(A) Identification of replicated HDL protein.** HDL proteins were presented by number of reported/publication times. 94 replicated human HDL proteins (published ≥ 2 times among 275 reported human HDL proteins), 72 replicated mouse HDL proteins (published ≥ 2 times among 111 reported mouse HDL proteins or replicated with our data) are presented. 12 replicated HDL proteins are identified (replicated ≥ 3 times in human and mouse proteomics) and framed in dash line. **(B) Strategy for the identification of 12 replicated HDL proteins. (C) Dynamic distribution of 12 replicated HDL proteins;** Relative abundance of each identified protein in HDL particles were described by relative peptide count determined by MS. A value of 1.0 was assigned to the highest peptide count in three S/M/L-HDL subclasses. Protein dynamic changes are expressed as peptide count curves. Identified HDL proteins were classified as increased, decreased and steadily expressed groups. Protein name abbreviation are explained in Table 1A. Standard abbreviations of HDL proteins were obtained from public databases (Genecards and Uniprot).

4. Discussion

During the process of RCT, HDL particles gradually mature and enlarge. HDL comprises a multitude of discrete proteins and differ in their composition, proteome and functional properties. In this study, we developed a strategy to classify HDL particles based on their size and to characterize the protein composition of these HDL subclasses. We identified 51 mouse HDL proteins and discovered 12 of them are replicated in previously published human and mouse HDL proteomes. We developed a model of protein composition change during HDL maturation and defined essential functions for all HDL particles as cholesterol efflux and immune response. Specifically for each subclass we determined special function of amino acid metabolism for S-HDL, anti-coagulation for M-HDL, and cholesterial clearance for L-HDL. We proposed that Pon1 is recruited into M/L-HDL to provide its anti-oxidatiove function. ApoE is incorporated into L-HDL to optimize its cholesterial clearance function.

We believe FPLC separation is a more effective method for HDL proteome study because FPLC isolation does not alter the analyzed substance. This retains most HDL protein components that might contribute to their heterogeneous functions. A traditional HDL isolation method is density gradient ultracentrifugation, which separates HDL

A Strategy of pathway/bio-function analysis of HDL proteins

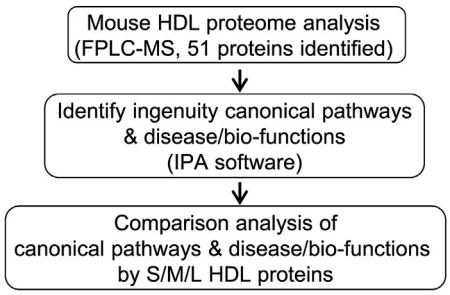

B Top 3 ingenuity pathways of S/M/L-HDL proteins

HDL subclasses (total identified)	Canonical pathways	*P Value*	Mol # (involved /total pathway)	% (involved mol. # /total identified)
Small (39)	LXR/RXR activation	5.33E-26	15/128	38.5
	FXR/RXR activation	1.74E-25	15/138	38.5
	Acute phase response	5.93E-22	14/171	35.9
Medium (27)	Acute phase response	3.12E-25	15/171	55.6
	LXR/RXR activation	2.95E-18	11/128	40.7
	FXR/RXR activation	6.19E-18	11/138	40.7
Large (29)	LXR/RXR activation	1.99E-20	12/128	41.4
	FXR/RXR activation	5.07E-20	12/138	41.4
	Acute phase response	6.10E-15	10/171	34.5

C Top 5 disease/bio-functions of S/M/L-HDL proteins

HDL subclasses (total identified)	Diseases/ bio-functions	*P* Value	Mol.# involved	% (involved mol. # /total identified)
Small (39)	Complement activation	1.82E-15	8	20.5
	Organ inflammation	3.55E-13	18	46.2
	Hemolysis	1.99E-12	8	20.5
	Cytolysis	3.14E-11	10	25.6
	Inflammation	5.35E-11	15	38.5
Medium (27)	Complement activation	2.01E-11	6	22.2
	inflammation	8.11E-11	15	55.6
	acute coronary syndrome	5.00E-10	8	29.6
	phospholipid efflux	6.83E-10	5	18.5
	myocardial infarction	5.76E-09	7	25.9
Large (29)	Complement activation	1.13E-13	7	24.1
	cholesterol efflux	3.88E-10	7	24.1
	phospholipid efflux	6.83E-10	5	17.2
	vascular disease	1.40E-09	13	44.8
	lipid homeostasis	7.47E-09	7	24.1

D Significance comparison of ingenuity pathways

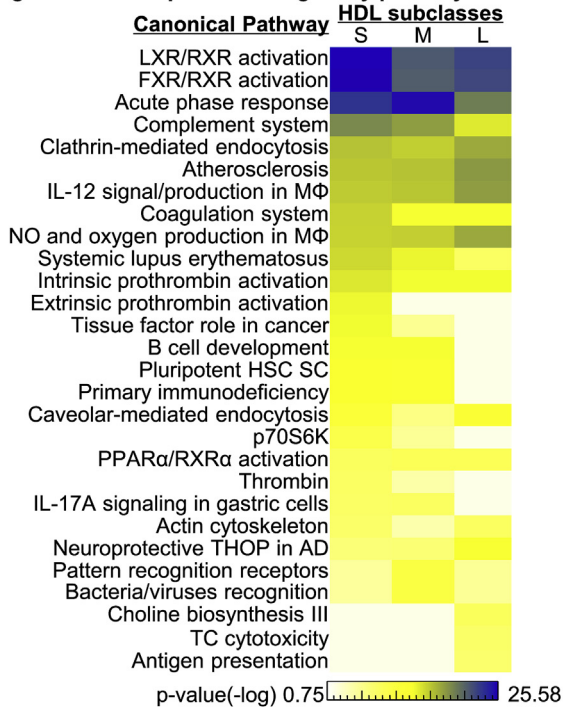

E Significance comparison of disease/bio-functions

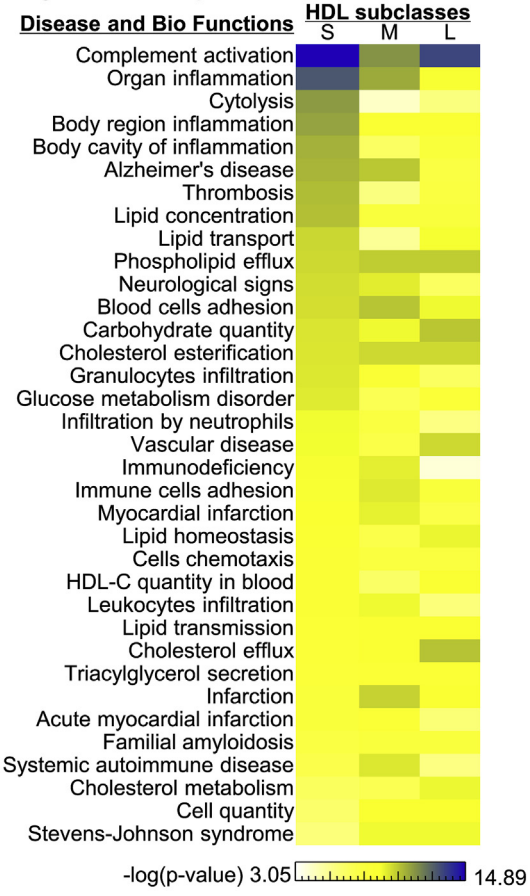

(caption on next page)

subfractions based on the buoyancy profile of lipoproteins using high-salt solutions and high centrifugal force. These extreme conditions increase the likelihood of denaturing the structural and chemical properties of HDL and removing associated proteins [26]. The drawback of the FPLC technique is the tendency towards fraction contamination with other plasma particles of similar sizes to that of HDL. For example, albumin overlapped with S-HDL and interfered with its fragmentation (Fig. 1B). This interference was resolved by PL and TC quantification,

Fig. 5. Identification of Ingenuity pathways & disease/bio-functions of HDL proteins and significance comparison (IPA software). 51 HDL proteins were identified by FPLC purification and MS analysis as described in Fig. 1 and Table 1. The abbreviation and Uniprot ID of these HDL proteins were obtained from public databases (Genecards and Uniprot) and used for the identification of Ingenuity pathways and disease/bio-functions (www.ingenuity.com). **(A) Strategy for pathway & function analysis of HDL proteins. (B) Top 3 ingenuity pathways of S/M/L-HDL proteins. (C) Top 5 disease/bio-functions of S/M/L HDL proteins.** The top 3 Ingenuity canonical pathways and top 5 disease/bio-functions of L/M/S-HDL particles were identified. The significance of identified pathways and disease/bio-functions were evaluated by *p*-value which describes the significance of individual pathway over others in each HDL fraction. Overlaps describe the numbers and percentage of identified HDL proteins in the previously identified pathway proteins. **(D) Heat map of significance comparison of ingenuity pathways. (E) Heat map of significance comparison of disease/bio-functions.** The significance comparison of Ingenuity pathways and disease/bio-functions between three HDL fractions was calculated as *P* value using IPA software and presented in the heat map. Blue color represents the highest significance (the smallest *p* value) of the identified pathway among three HDL fractions. White color represents the lowest significance (the largest *p* value) among three fractions. Abbreviations: AD, Alzheimer's disease; defi., deficiency; HSC, hematopoiesis; MΦ, macrophage; NO, nitric oxide; R, Receptor; ROS, reactive oxygen species; SC, stem cell; TC, targeted cell, T1DM, type 1 diabetes mellitus. (For interpretation of the references to color in this figure legend, the reader is referred to the Web version of this article.)

A Strategy of network identification of HDL proteins

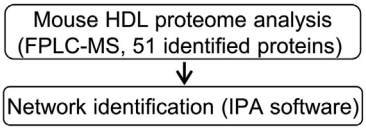

B Three networks for HDL populations (IPA software)

HDL subclass (total identified)	IPA Score	Involved mol. # (% of Involved/total identified)	Associated diseases and functions
Small (39 proteins)	**59**	22 (56.4)	Humoral Immune Response, Inflammatory Response, Carbohydrate Metabolism
	10	5(12.8)	Cellular Assembly and Organization, Tissue Development, Cellular Function and Maintenance
	2	1(0.03)	Post-Translational Modification, Organismal Injury and Abnormalities, Reproductive System Disease
Medium (27 proteins)	**59**	21(77.8)	Developmental Disorder, Hereditary Disorder, Immunological Disease
	7	4(14.8)	Cell Death and Survival, Cellular Compromise, Cellular Development
	2	1(0.07)	Cardiovascular Disease, Hematological Disease, Energy Production
Large (29 proteins)	**59**	21(72.4)	Cell Death and Survival, Connective Tissue Disorders, Hematological Disease
	14	7(24.1)	Lipid Metabolism, Small Molecule Biochemistry, Drug Metabolism
	3	2(0.07)	Cell Signaling, Post-Translational Modification, Organ Morphology

C Molecular property of network proteins

Symbol	Molecular	Symbol	Molecular
	Phosphatase		Other
	Peptidase		Group/Complex
	Enzyme		Transmembrane receptor
	Transporter		Relationship

D S-HDL top network (IPA score 59)

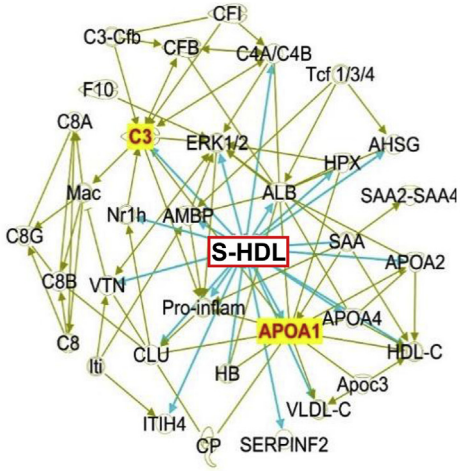

E Top M-HDL network (IPA score 59)

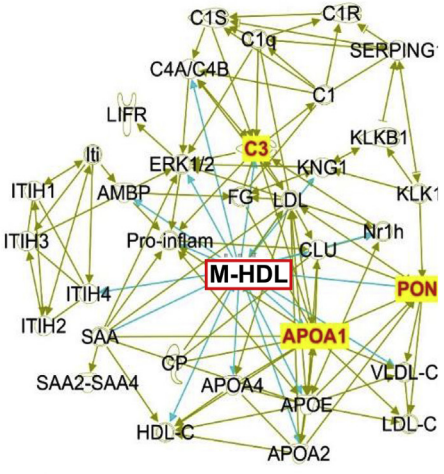

F Top L-HDL network (IPA score 59)

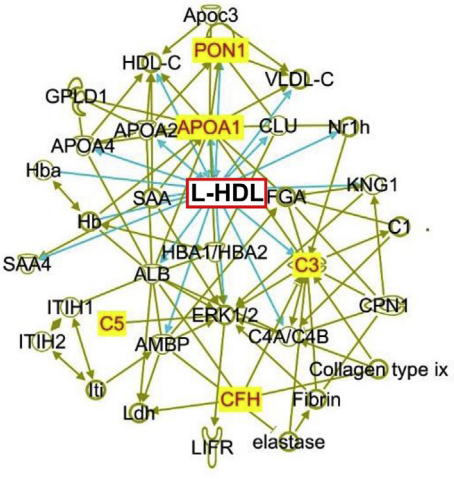

Fig. 6. Network identification of HDL proteins (IPA software). (A) Strategy of network identification. 51 HDL proteins (39 in S-HDL, 27 in M-HDL, and 29 in L-HDL) were identified in mouse plasma by FPLC purification and MS analysis as describing in Fig. 1 and Table 1 and used for network analyzing by IPA software (www.ingenuity.com). Predicted networks and score are calculated using IPA algorithm. Each connection represents known relationships between the molecules found in the Ingenuity knowledge base. **(B) Top 3 networks for each HDL population.** The top 3 scored networks and their associated diseases/bio-functions of L/M/S-HDL are presented. **(C) Molecular property of network proteins. (D) S-HDL top network. (E) M-HDL top network. (F). L-HDL top network.** The highest scored networks for S/M/L-HDL subclasses are presented. Blue lines indicate direct interactions of 2 molecules. Green lines indicate indirect interactions. The symbols describe the property of the molecules and explained in **C.** Abbreviations for identified HDL proteins are explained in Table 1A. (For interpretation of the references to color in this figure legend, the reader is referred to the Web version of this article.)

which precisely distinguished HDL (Fig. 1C/D). Another special advantage of the FPLC technique is the ability to further precisely fractionate HDL subgroups, which allows for accurate quantitative chemical and molecular analysis of our fractions. Using these advanced technologies in combination with FPLC and lipid chemical analysis, we obtained well-separated HDL fractions and, for the first time, analyzed the proteome and major lipid components of pooled S/M/L-HDL subpopulations. We found that protein concentration in L/M-HDL was 6-fold lower than those in S-HDL (0.1–0.4–1.4 mg/ml) (Fig. 1F). PL, TC and TG were enriched by approximately 7-, 10- and 20-fold in L/M-HDL over S-HDL (25–34 to 3 μg/mg, 14–20 to 3 μg/mg, 1.5–1.7 to 0.25 μg/mg) (Fig. 1G/H/I). These data provided quantitative information to support the theory of increased lipid and decreased protein content during HDL maturation [27]. We identified 10/27 different proteins in L/M-HDL and 39 proteins in S-HDL(Fig. 2), suggesting that the high protein content in S-HDL is, at least in part, related to its abundance of protein constituents. It is likely that various protein constituents in S-HDL determine its diverse functions, described as follows.

Our mouse HDL subclass proteome on FPLC-derived S/M/L-HDL subclasses displayed differential composition and dynamic change of protein components during HDL maturation; leading us to propose that HDL protein component determines the diversed biological function of diefferent HDL subclasses. We found that, in general, the 39 S-HDL proteins modulate cholesterol efflux, immune response and amino acid metabolism. M-HDL and L-HDL contain fewer proteins (27 and 29) and carry out anti-inflammation and antioxidation roles, in addition to cholesterol efflux and immune responses. M-HDL is specifically associated with anticoagulation function. These novel findings suggest that differential protein composition and dynamic changes in the HDL subpopulation may better reflect HDL functions than HDL-C levels.

We identified 10 complement proteins in HDL fractions. C5 and CFH had very low levels in S-HDL but become highly expressed in L-HDL. In contrast, the other 8 complement proteins (C3, C4B, C8A, C8B, C8G, CFB, CFI and Clu) were highly expressed in S-HDL but almost disappeared in L-HDL. HDL has been recognized as a carrier of complement proteins in humans and has been shown to contain C1q, C1s, C2, C3, C4, C5, C9, FB, FH, and C1–INH [17,28,29]. As a part of the innate immune system, complement activation results in the formation of the cell-killing membrane attack complex [30]. Over 30 different proteins have been implicated in the complement pathway. At least 17 of these proteins have been found to bind to HDL, supporting the concept of HDL involvement in complement regulation [31]. We found that CFH, a complement inhibitor protein, is greatly increased in L-HDL (Fig. 3B1). The enrichment of CFH in L-HDL may explain the ability of HDL to prevent the organization of complement membrane attack complex [32,33] and to suppress inflammation. The 8 S-HDL enriched complement proteins (Fig. 3B1) may contribute to the immune/inflammatory function of S-HDL suggested in this study. It is likely that S-HDL participates in complement activation, phagocytosis, pathogen elimination and the inflammatory response. Complement system activation has been linked to CVD and metabolic complications, potentially via its cytolysis effect [32]. Studies in our laboratory are currently being performed to test whether complement protein-enriched S-HDL is harmful to biological systems.

Among inflammation-related proteins (Fig. 3B2), we found that Ambp, ItiH1, and ItiH2 were increased in M/L-HDL, whereas ItiH3 and ItiH4 were reduced. These proteins are implicated in adhesion, ligand binding/uptake by scavenger receptors and may be responsible for the interaction between M/L-HDL and cells independent of apolipoproteins. Importantly, Pon1, a well-characterized antioxidation protein, appeared only in M/L-HDL. Pon1 is known for its HDL-associated antioxidant capacity [34]. Reduced Pon1 activity is associated with increased oxidative stress and CVD in humans and with atherogenesis in mice [28,35,36]. This finding suggests that HDL antioxidant capacity [34]is present only in M/L-HDL, not in S-HDL. In addition, we identified an abundance of Saa4 in S-HDL only. Since Saa4 is an acute phase protein associated with folate metabolism [37], which is a key remethylation pathway for methionine-homocysteine metabolism, S-HDL may participate in regulating amino acid and methylation metabolism.

We found 7 immunoglobulins favorably expressed in S-HDL, reduced in M-HDL, and absent in L-HDL (Fig. 3B3). The 8 S-HDL-enriched complement proteins exhibited a similar pattern. This further supports the role of S-HDL in complement activation and innate and adaptive immune regulation. We identified 7 HDL-associated coagulation proteins, including 2 pro-coagulating proteins (F10 and F2) and 5 anticoagulating proteins (Klkb1, Kng1 and Serpina1/2/10) (Fig. 3C). All proteins were present at relatively low concentrations in L-HDL. This insinuates that HDL particles, or at least L-HDL particles, do not play important roles in coagulation and thrombotic regulation. We identified 13 HDL-associated proteins with diverse functions and classified them as other types of proteins (Fig. 3D). This heterogeneity of diverse proteins in HDL subfractions suggests alternative functions for different HDL subfractions and highlights the need for further molecular studies.

We presented a model for HDL protein exchange during HDL biosynthesis in Fig. 3E and summarized 3 important major features for mouse HDL protein dynamic changes. 1) All HDL subfractions contain ApoA1/A2/A4, while only L-HDL contains ApoE. 2) All activating complement proteins are present in S-HDL, but the inhibitory complement protein CFH is expressed only in L-HDL. 3) Pon1 is present in M-HDL and L-HDL. It is known that ApoE mediates cholesterol liver uptake via the LDL receptor and suppresses the TC- and MC-related inflammation response [38,39], consistent with previously reported data showing the lack of functional HDL in ApoE knockout mice.

We believe that HDL protein dynamic changes determine the heterogeneous functions of HDL subpopulations. Considering the overall protein dynamic changes in S/M/L-HDL, we proposed three major functions for each HDL subpopulation. The S-HDL fraction mostly regulates cholesterol efflux, the immune response and amino acid metabolism. The M-HDL fraction maintains cholesterol efflux and immune response functions and shows new antioxidation and anticoagulation functions, attributable to the incorporation of Pon1 and the anticoagulation proteins Klkb1, Serpina10, Kng, and Serping1. L-HDL is likely the most protective HDL population. It remains as powerful as M-HDL in cholesterol efflux and antioxidation but shows enhanced functions in cholesterol liver uptake and anti-inflammation, mostly due to the dominant expression of the ApoE, CFH and Pon1 proteins. This is consistent with knowledge of the antioxidative and anti-inflammatory functions of Pon1, the complement suppression functions of CFH, and the cholesterol liver uptake and anti-inflammatory functions of ApoE [38,40–42]. Our findings emphasize three major functions determined by HDL proteins: lipid transport, immune regulation and antioxidation. Our data provide evidence of HDL heterogeneity in protein composition and a connection with the biological functions of HDL subfractions of different sizes. Studies in our laboratory are undergoing to validate the biological effects of these different HDL subclasses.

We compared our findings with a few representative HDL proteomic studies [17,23,43–51] (Supplementary Table 2) and identified 12 replicated proteins in human and mouse HDL that overlapped with our proteomics results and were reported at least twice in previous HDL proteomic studies (Fig. 4A/B). Our HDL subclass proteomic dataset is the first used to evaluate structural and functional connections and contributions to HDL heterogeneity using replicated HDL proteins in both humans and mice. We found that the replicated HDL proteins PON1, C5 and ApoE increased during HDL maturation, which largely determines the antioxidation, anti-inflammation and cholesterol clearance functions acquired during HDL biosynthesis in both humans and mice (Fig. 4C). Importantly, ApoA1, ApoA2 and ApoC3 were steadily expressed in all HDL subclasses, which is critical for maintaining essential cholesterol efflux functions for all HDL populations. The functional implications of C3, Saa4, Vtn, CP and ApoA4, which were gradually reduced during HDL maturation, require further analysis. Our study aimed to classify the similarity between mouse and human HDL

proteome and provided rationale for using mouse model to study HDL proteomics and lipoproteomics in human disease. Research to investigate human HDL protein dynamics in HDL subclasses and in disease conditions are on-going in our laboratory, and will be published in separate manuscripts in the near future.

Our Ingenuity pathway analysis described 3 top pathways (LXR/RXR activation, FXR/RXR activation, and acute phase response) ($p \leq 7.94E-09$) that were similarly present in all three HDL subfractions (Fig. 5B) and 5 top disease/bio-functions differentially related to S/M/L-HDL subclasses (Fig. 5C). Our findings highlighted the functions of HDL subclasses, especially S-HDL, in LXR/RXR and FXR/RXR activation, suggesting a novel function of HDL in the trans-activation of lipid metabolism and cholesterol to bile acid catabolism. The HDL acute phase response pathway is most likely mediated by the complement system, since we identified 10 complement proteins as mouse HDL constituents. Complement activation is the fourth pathway and the first disease function of HDL identified by Ingenuity pathway analysis (Fig. 5D/E).

In this study, we used male mice to eliminate the influence of sex steroid. It is established that lower estrogen levels is associated with higher morbidity of coronary heart disease and lower HDL-C levels in human [52,53]. Gender effect on HDL subclass was also reported. Males have lower HDL2-C and HDL3-C subtraction [55]. Greater declines in estrogen E2 were associated with large increases in S-HDL-PIMA and reductions in M-HDL-PIMA in healthy women tansitioning through Menopause [56]. However, information regarding gender effect on HDL proteomics is not currently not available. It is likely that sex steroid effect HDL proteomics and function, which is an interesting topic for future studies.

In conclusion, our current study provided the first HDL subclass proteomics. We identified 51 proteins in three mouse S/M/L-HDL subclasses, and characterized their dynamic changes during HDL maturation. We discovered 5 apolipoproteins (A1, A2, A4, C3 and E) that possess cholesterol efflux and anti-inflammatory functions and 10 complement and 7 immunoglobin proteins that mostly contribute to immune response and anti-inflammatory functions. We propose cholesterol efflux and immune response as the essential functions for all HDL particles, amino acid metabolism as a special function of S-HDL, and anti-coagulation as a special function for M-HDL. Pon1 is recruited into M/L-HDL to precess its antioxidatiove function because Pon1 appears only in M/L-HDL. ApoE is incoerperated into L-HDL to optimize its cholesterial clearance function because ApoE was only detected in L-HDL. Our discoveries provide a novel basis of HDL structural and functional heterogeneity and suggest that HDL is a powerful molecular vehicle for multisystem metabolic and molecular regulation and is an accessible therapeutic target.

5. Disclosures

None.

Acknowledgements

This work was supported in part by the National Institutes of Health grants HL67033, HL77288, HL82774, HL-110764, HL130233, HL131460, DK104114, DK113775 to HW and HL131460 to HW/EC/XFY. YLZ is supported by a fellowship from China Scholarship Council.

The authors acknowledge the contributions of Huimin Shan from Temple University, for animal care and part of the sample collection, and James M Dipaul from Temple University, for part of the technical assistance with FPLC (Bio-Rad, Duo flow) settings.

The content is solely the responsibility of the authors and does not necessarily represent the official views of the National Institutes of Health.

Appendix A. Supplementary data

Supplementary data to this article can be found online at https://doi.org/10.1016/j.redox.2019.101222.

References

[1] N.J. Stone, J.G. Robinson, A.H. Lichtenstein, C.N. Bairey Merz, C.B. Blum, R.H. Eckel, A.C. Goldberg, D. Gordon, D. Levy, D.M. Lloyd-Jones, P. McBride, J.S. Schwartz, S.T. Shero, S.C. Smith Jr., K. Watson, P.W. Wilson, K.M. Eddleman, N.M. Jarrett, K. LaBresh, L. Nevo, J. Wnek, J.L. Anderson, J.L. Halperin, N.M. Albert, B. Bozkurt, R.G. Brindis, L.H. Curtis, D. DeMets, J.S. Hochman, R.J. Kovacs, E.M. Ohman, S.J. Pressler, F.W. Sellke, W.K. Shen, G.F. Tomaselli, 2013 ACC/AHA guideline on the treatment of blood cholesterol to reduce atherosclerotic cardiovascular risk in adults: a report of the American College of Cardiology/American Heart Association Task Force on practice guidelines, Circulation 129 (2014) S1–S45.

[2] A.M. Lincoff, S.J. Nicholls, J.S. Riesmeyer, P.J. Barter, H.B. Brewer, K.A.A. Fox, C.M. Gibson, C. Granger, V. Menon, G. Montalescot, D. Rader, A.R. Tall, E. McErlean, K. Wolski, G. Ruotolo, B. Vangerow, G. Weerakkody, S.G. Goodman, D. Conde, D.K. McGuire, J.C. Nicolau, J.L. Leiva-Pons, Y. Pesant, W. Li, D. Kandath, S. Kouz, N. Tahirkheli, D. Mason, S.E. Nissen, A. Investigators, Evacetrapib and cardiovascular outcomes in high-risk vascular disease, N. Engl. J. Med. 376 (2017) 1933–1942.

[3] F.H. Rached, M.J. Chapman, A. Kontush, HDL particle subpopulations: focus on biological function, Biofactors 41 (2015) 67–77.

[4] D. Liao, X. Yang, H. Wang, Hyperhomocysteinemia and high-density lipoprotein metabolism in cardiovascular disease, Clin. Chem. Lab. Med. 45 (2007) 1652–1659.

[5] D. Liao, H. Tan, R. Hui, Z. Li, X. Jiang, J. Gaubatz, F. Yang, W. Durante, L. Chan, A.I. Schafer, H.J. Pownall, X. Yang, H. Wang, Hyperhomocysteinemia decreases circulating high-density lipoprotein by inhibiting apolipoprotein A-I Protein synthesis and enhancing HDL cholesterol clearance, Circ. Res. 99 (2006) 598–606.

[6] S. Sankaranarayanan, J.F. Oram, B.F. Asztalos, A.M. Vaughan, S. Lund-Katz, M.P. Adorni, M.C. Phillips, G.H. Rothblat, Effects of acceptor composition and mechanism of ABCG1-mediated cellular free cholesterol efflux, J. Lipid Res. 50 (2009) 275–284.

[7] M. de la Llera-Moya, D. Drazul-Schrader, B.F. Asztalos, M. Cuchel, D.J. Rader, G.H. Rothblat, The ability to promote efflux via ABCA1 determines the capacity of serum specimens with similar high-density lipoprotein cholesterol to remove cholesterol from macrophages, Arterioscler. Thromb. Vasc. Biol. 30 (2010) 796–801.

[8] F.M. Sacks, L.L. Rudel, A. Conner, H. Akeefe, G. Kostner, T. Baki, G. Rothblat, M. de la Llera-Moya, B. Asztalos, T. Perlman, C. Zheng, P. Alaupovic, J.A. Maltais, H.B. Brewer, Selective delipidation of plasma HDL enhances reverse cholesterol transport in vivo, J. Lipid Res. 50 (2009) 894–907.

[9] D.J. Rader, E.T. Alexander, G.L. Weibel, J. Billheimer, G.H. Rothblat, The role of reverse cholesterol transport in animals and humans and relationship to atherosclerosis, J. Lipid Res. 50 (Suppl) (2009) S189–S194.

[10] R.J. Havel, H.A. Eder, J.H. Bragdon, The distribution and chemical composition of ultracentrifugally separated lipoproteins in human serum, J. Clin. Investig. 34 (1955) 1345–1353.

[11] G. Kostner, P. Alaupovic, Studies of the composition and structure of plasma lipoproteins. C- and N-terminal amino acids of the two nonidentical polypeptides of human plasma apolipoprotein A, FEBS Lett. 15 (1971) 320–324.

[12] R.W. Mahley, T.L. Innerarity, Interaction of canine and swine lipoproteins with the low density lipoprotein receptor of fibroblasts as correlated with heparin/manganese precipitability, J. Biol. Chem. 252 (1977) 3980–3986.

[13] M. Ayrault-Jarrier, J.F. Alix, J. Polonovski, [Presence and isolation of 2 lipoproteins immunologically related to apolipoprotein A I in human serum], Biochimie 62 (1980) 51–59.

[14] C.A. Vezina, R.W. Milne, P.K. Weech, Y.L. Marcel, Apolipoprotein distribution in human lipoproteins separated by polyacrylamide gradient gel electrophoresis, J. Lipid Res. 29 (1988) 573–585.

[15] M.C. Blatter, R.W. James, S. Messmer, F. Barja, D. Pometta, Identification of a distinct human high-density lipoprotein subspecies defined by a lipoprotein-associated protein, K-45. Identity of K-45 with paraoxonase, Eur. J. Biochem. 211 (1993) 871–879.

[16] R.S. Rosenson, H.B. Brewer Jr., M.J. Chapman, S. Fazio, M.M. Hussain, A. Kontush, R.M. Krauss, J.D. Otvos, A.T. Remaley, E.J. Schaefer, HDL measures, particle heterogeneity, proposed nomenclature, and relation to atherosclerotic cardiovascular events, Clin. Chem. 57 (2011) 392–410.

[17] S.M. Gordon, J. Deng, L.J. Lu, W.S. Davidson, Proteomic characterization of human plasma high density lipoprotein fractionated by gel filtration chromatography, J. Proteome Res. 9 (2010) 5239–5249.

[18] S.M. Gordon, J. Deng, A.B. Tomann, A.S. Shah, L.J. Lu, W.S. Davidson, Multi-dimensional co-separation analysis reveals protein-protein interactions defining plasma lipoprotein subspecies, Mol. Cell. Proteom. 12 (2013) 3123–3134.

[19] M. O'Reilly, E. Dillon, W. Guo, O. Finucane, A. McMorrow, A. Murphy, C. Lyons, D. Jones, M. Ryan, M. Gibney, E. Gibney, L. Brennan, M. de la Llera Moya, M.P. Reilly, H.M. Roche, F.C. McGillicuddy, High-density lipoprotein proteomic composition, and not efflux capacity, reflects differential modulation of reverse cholesterol transport by saturated and monounsaturated fat diets, Circulation 133 (2016) 1838–1850.

[20] T. Padro, J. Cubedo, S. Camino, M.T. Bejar, S. Ben-Aicha, G. Mendieta, J.C. Escola-Gil, R. Escate, M. Gutierrez, L. Casani, L. Badimon, G. Vilahur, Detrimental effect of

hypercholesterolemia on high-density lipoprotein particle remodeling in pigs, J. Am. Coll. Cardiol. 70 (2017) 165–178.
[21] W.S. Davidson, R.A. Silva, S. Chantepie, W.R. Lagor, M.J. Chapman, A. Kontush, Proteomic analysis of defined HDL subpopulations reveals particle-specific protein clusters: relevance to antioxidative function, Arterioscler. Thromb. Vasc. Biol. 29 (2009) 870–876.
[22] M.C. Camus, M.J. Chapman, P. Forgez, P.M. Laplaud, Distribution and characterization of the serum lipoproteins and apoproteins in the mouse, Mus musculus, J. Lipid Res. 24 (1983) 1210–1228.
[23] S.M. Gordon, H. Li, X. Zhu, A.S. Shah, L.J. Lu, W.S. Davidson, A comparison of the mouse and human lipoproteome: suitability of the mouse model for studies of human lipoproteins, J. Proteome Res. 14 (2015) 2686–2695.
[24] S.M. Gordon, H. Li, X. Zhu, A.S. Shah, L.J. Lu, W.S. Davidson, A comparison of the mouse and human lipoproteome: suitability of the mouse model for studies of human lipoproteins, J. Proteome Res. 14 (6) (2015 June 5) 2686–2695, https://doi.org/10.1021/acs.jproteome.5b00213.
[25] W.S. Davidson, R.A. Silva, S. Chantepie, W.R. Lagor, M.J. Chapman, A. Kontush, Proteomic analysis of defined HDL subpopulations reveals particle-specific protein clusters: relevance to antioxidative function, Arterioscler. Thromb. Vasc. Biol. 29 (2009) 870–876.
[26] F. van't Hooft, R.J. Havel, Metabolism of apolipoprotein E in plasma high density lipoproteins from normal and cholesterol-fed rats, J. Biol. Chem. 257 (1982) 10996–11001.
[27] L. Tian, Y. Xu, M. Fu, T. Peng, Y. Liu, S. Long, The impact of plasma triglyceride and apolipoproteins concentrations on high-density lipoprotein subclasses distribution, Lipids Health Dis. 10 (2011) 17.
[28] T. Vaisar, S. Pennathur, P.S. Green, S.A. Gharib, A.N. Hoofnagle, M.C. Cheung, J. Byun, S. Vuletic, S. Kassim, P. Singh, H. Chea, R.H. Knopp, J. Brunzell, R. Geary, A. Chait, X.Q. Zhao, K. Elkon, S. Marcovina, P. Ridker, J.F. Oram, J.W. Heinecke, Shotgun proteomics implicates protease inhibition and complement activation in the antiinflammatory properties of HDL, J. Clin. Investig. 117 (2007) 746–756.
[29] F. Rezaee, B. Casetta, J.H. Levels, D. Speijer, J.C. Meijers, Proteomic analysis of high-density lipoprotein, Proteomics 6 (2006) 721–730.
[30] C.A. Janeway, P. Traver, M. Walport, M. Shlomchik, Immunobiology: the Immune System in Health and Disease, Garland Science, New York, 2005.
[31] S.M. Gordon, A.T. Remaley, High density lipoproteins are modulators of protease activity: implications in inflammation, complement activation, and atherothrombosis, Atherosclerosis 259 (2017) 104–113.
[32] K.K. Hamilton, J. Zhao, P.J. Sims, Interaction between apolipoproteins A-I and A-II and the membrane attack complex of complement. Affinity of the apoproteins for polymeric C9, J. Biol. Chem. 268 (1993) 3632–3638.
[33] S.I. Rosenfeld, C.H. Packman, J.P. Leddy, Inhibition of the lytic action of cell-bound terminal complement components by human high density lipoproteins and apoproteins, J. Clin. Investig. 71 (1983) 795–808.
[34] H. Soran, J.D. Schofield, Y. Liu, P.N. Durrington, How HDL protects LDL against atherogenic modification: paraoxonase 1 and other dramatis personae, Curr. Opin. Lipidol. 26 (2015) 247–256.
[35] T. Bhattacharyya, S.J. Nicholls, E.J. Topol, R. Zhang, X. Yang, D. Schmitt, X. Fu, M. Shao, D.M. Brennan, S.G. Ellis, M.L. Brennan, H. Allayee, A.J. Lusis, S.L. Hazen, Relationship of paraoxonase 1 (PON1) gene polymorphisms and functional activity with systemic oxidative stress and cardiovascular risk, J. Am. Med. Assoc. 299 (2008) 1265–1276.
[36] D.M. Shih, A.J. Lusis, The roles of PON1 and PON2 in cardiovascular disease and innate immunity, Curr. Opin. Lipidol. 20 (2009) 288–292.
[37] S.C. van Dijk, A.W. Enneman, K.M. Swart, J.P. van Wijngaarden, A.C. Ham, R. de Jonge, H.J. Blom, E.J. Feskens, J.M. Geleijnse, N.M. van Schoor, R.A. Dhonukshe-Rutten, R.T. de Jongh, P. Lips, L.C. de Groot, A.G. Uitterlinden, T.H. van den Meiracker, F.U. Mattace-Raso, N. van der Velde, Y.M. Smulders, Effect of vitamin B12 and folic acid supplementation on biomarkers of endothelial function and inflammation among elderly individuals with hyperhomocysteinemia, Vasc. Med. 21 (2016) 91–98.
[38] D.J. Christensen, N. Ohkubo, J. Oddo, M.J. Van Kanegan, J. Neil, F. Li, C.A. Colton, M.P. Vitek, Apolipoprotein E and peptide mimetics modulate inflammation by binding the SET protein and activating protein phosphatase 2A, J. Immunol. 186 (2011) 2535–2542.
[39] K. Li, D. Ching, F.S. Luk, R.L. Raffai, Apolipoprotein E enhances microRNA-146a in monocytes and macrophages to suppress nuclear factor-kappaB-driven inflammation and atherosclerosis, Circ. Res. 117 (2015) e1–e11.
[40] A.P. Herbert, E. Makou, Z.A. Chen, H. Kerr, A. Richards, J. Rappsilber, P.N. Barlow, Complement evasion mediated by enhancement of captured factor H: implications for protection of self-surfaces from complement, J. Immunol. 195 (2015) 4986–4998.
[41] J. Kotur-Stevuljevic, S. Spasic, Z. Jelic-Ivanovic, V. Spasojevic-Kalimanovska, A. Stefanovic, A. Vujovic, L. Memon, D. Kalimanovska-Ostric, PON1 status is influenced by oxidative stress and inflammation in coronary heart disease patients, Clin. Biochem. 41 (2008) 1067–1073.
[42] Y. Kumon, T. Suehiro, Y. Ikeda, K. Hashimoto, Human paraoxonase-1 gene expression by HepG2 cells is downregulated by interleukin-1beta and tumor necrosis factor-alpha, but is upregulated by interleukin-6, Life Sci. 73 (2003) 2807–2815.
[43] S.M. Gordon, W.S. Davidson, E.M. Urbina, L.M. Dolan, A. Heink, H. Zang, L.J. Lu, A.S. Shah, The effects of type 2 diabetes on lipoprotein composition and arterial stiffness in male youth, Diabetes 62 (2013) 2958–2967.
[44] Y. Jin, S. Bu, J. Zhang, Q. Yuan, T. Manabe, W. Tan, Native protein mapping and visualization of protein interactions in the area of human plasma high-density lipoprotein by combining nondenaturing micro 2DE and quantitative LC-MS/MS, Electrophoresis 35 (2014) 2055–2064.
[45] I. Jorge, E. Burillo, R. Mesa, L. Baila-Rueda, M. Moreno, M. Trevisan-Herraz, J.C. Silla-Castro, E. Camafeita, M. Ortega-Munoz, E. Bonzon-Kulichenko, I. Calvo, A. Cenarro, F. Civeira, J. Vazquez, The human HDL proteome displays high inter-individual variability and is altered dynamically in response to angioplasty-induced atheroma plaque rupture, J Proteomics 106 (2014) 61–73.
[46] M.N. Martinez, C.H. Emfinger, M. Overton, S. Hill, T.S. Ramaswamy, D.A. Cappel, K. Wu, S. Fazio, W.H. McDonald, D.L. Hachey, D.L. Tabb, J.M. Stafford, Obesity and altered glucose metabolism impact HDL composition in CETP transgenic mice: a role for ovarian hormones, J. Lipid Res. 53 (2012) 379–389.
[47] M. Riwanto, L. Rohrer, B. Roschitzki, C. Besler, P. Mocharla, M. Mueller, D. Perisa, K. Heinrich, L. Altwegg, A. von Eckardstein, T.F. Luscher, U. Landmesser, Altered activation of endothelial anti- and proapoptotic pathways by high-density lipoprotein from patients with coronary artery disease: role of high-density lipoprotein-proteome remodeling, Circulation 127 (2013) 891–904.
[48] I. Sreckovic, R. Birner-Gruenberger, C. Besenboeck, M. Miljkovic, T. Stojakovic, H. Scharnagl, G. Marsche, U. Lang, J. Kotur-Stevuljevic, Z. Jelic-Ivanovic, G. Desoye, C. Wadsack, Gestational diabetes mellitus modulates neonatal high-density lipoprotein composition and its functional heterogeneity, Biochim. Biophys. Acta 1841 (2014) 1619–1627.
[49] Y. Tan, T.R. Liu, S.W. Hu, D. Tian, C. Li, J.K. Zhong, H.G. Sun, T.T. Luo, W.Y. Lai, Z.G. Guo, Acute coronary syndrome remodels the protein cargo and functions of high-density lipoprotein subfractions, PLoS One 9 (2014) e94264.
[50] A. von Zychlinski, M. Williams, S. McCormick, T. Kleffmann, Absolute quantification of apolipoproteins and associated proteins on human plasma lipoproteins, J Proteomics 106 (2014) 181–190.
[51] H.N. Yassine, A.M. Jackson, C.R. Borges, D. Billheimer, H. Koh, D. Smith, P. Reaven, S.S. Lau, C.H. Borchers, The application of multiple reaction monitoring and multi-analyte profiling to HDL proteins, Lipids Health Dis. 13 (2014) 8.
[52] T. Gordon, W.B. Kannel, M.C. Hjortland, P.M. McNamara, Menopause and coronary heart disease. The Framingham study, Ann. Intern. Med. 89 (1978) 157–161.
[53] V.H. Goh, T.Y. Tong, H.P. Mok, B. Said, Differential impact of aging and gender on lipid and lipoprotein profiles in a cohort of healthy Chinese Singaporeans, Asian J. Androl. 9 (2007) 787–794.
[55] P. Anagnostis, J.C. Stevenson, D. Crook, D.G. Johnston, I.F. Godsland, Effects of menopause, gender and age on lipids and high-density lipoprotein cholesterol subfractions, Maturitas 81 (2015) 62–68.
[56] S.R. El Khoudary, P.M. Hutchins, K.A. Matthews, M.M. Brooks, T.J. Orchard, G.E. Ronsein, J.W. Heinecke, Cholesterol efflux capacity and subclasses of HDL particles in healthy women transitioning through menopause, J. Clin. Endocrinol. Metab. 101 (2016) 3419–3428.